X005

Importance of Azimuth Data for 3D Inversion of Marine CSEM Scanning Data

J.P. Morten (Electromagnetic Geoservices ASA), A.K. Bjørke (Electromagnetic Geoservices ASA), T. Støren (Electromagnetic Geoservices ASA), E. Coward* (Electromagnetic Geoservices ASA), S.A. Karlsen (Electromagnetic Geoservices ASA) & F. Roth (Electromagnetic Geoservices ASA)

SUMMARY

We present 3D inversion results of synthetic, marine controlled-source electromagnetic (CSEM) data for a coarse receiver grid and a denser receiver grid. The coarse receiver grid, 4 km by 4 km, is representative for a scanning survey employed to detect prospects over large areas, whereas the denser receiver grid, 2 km by 2 km, is suitable for a more detailed characterization of known prospects. The results indicate that by including azimuth data, it is possible to detect resistors from scanning dataset even if the resistors are located between the coarse grid towlines. We then show how the fine details of identified resistors are resolved by inversion of a denser grid dataset.

Introduction

Marine controlled-source electromagnetic (CSEM) measurements are sensitive to the electric resistivity distribution in the subsurface, and are becoming a standard tool for offshore petroleum prospect ranking (Constable and Srnka, 2007). Traditionally, one or a few lines of receivers are deployed on the seabed and a powerful electric dipole source is towed over these lines. Anomalous responses in the recorded electromagnetic fields with respect to a reference measurement can indicate the presence of hydrocarbon-saturated sediments. Lower dimensional inversion approaches, like common midpoint inversion and 2.5D inversion, have been applied successfully for reservoir imaging using line data (Mittet et al., 2008; Abubakar et al., 2008). However, 3D effects can invalidate such approaches and demand 3D inversion to obtain a reliable model of the subsurface resistivity distribution. A full 3D model description also makes it possible to include data from receivers located off the active source towline in survey grids. In this paper, we demonstrate how the additional information gathered by such azimuth receivers in 3D survey grids accommodates inversion of data from a scanning survey layout where the receiver separation is large (> 2 km). Moreover, we show how data from a denser grid provide additional details in the resistor reconstruction.

3D survey layouts and azimuth data

CSEM acquisition where receivers are deployed in grids is now becoming the standard survey type. An advantageous feature of these surveys is the additional information obtained from data recorded by azimuth receivers. Azimuth data can be recorded by letting several receiver lines record data for each source line towing. This substantially increases the amount of data gathered compared to 2D line-type surveys where only receivers inline with the source towline record data. The azimuth data can be interpreted within the established workflows of normalization against a reference measurement using a decomposition technique that estimates the inline component of the data (Thrane et al., 2007). This provides data points that can be displayed between source towlines in the midpoint-offset domain. However, to make complete use of the data from a 3D survey, a more advanced processing technique is required. Data inversion in 3D could be the ultimate data processing tool for 3D survey datasets, since it can make use of data points for any source or receiver position and orientation. Moreover, information embedded in both measured horizontal field components is utilized. The inversion algorithm provides resistivity distribution models for detection of high-resistive hydrocarbon volumes, as well as information about the formation background resistivity. Specifically for 3D surveys, the additional data provided by azimuth receivers is more sensitive to horizontal components of the electromagnetic vector fields interacting with the 3D resistivity distribution. This gives information about anisotropy (Jing et al., 2008), which cannot be obtained by line surveys and lower dimensional inversion approaches.

In scanning surveys, the receiver layouts are typically coarse and cover large areas (Suffert et al., 2008). The receiver spacing is such that the data acquired will be sufficient to detect any substantial resistive bodies, yet cost-efficient to cover a large area. Such datasets are challenging cases for inversion, which typically requires dense sets of data points to give enough information for a detailed imaging procedure. However, by properly including the data recorded by azimuth receivers, we will show that the scanning survey data can be used for resistor imaging and detection at reasonable detail. An important requirement is that the noise levels are low enough to provide useful data from azimuth receiver lines separated by several kilometres from the source towline. Identified resistive targets in the model can then be imaged accurately by inversion of a subsequently acquired dense survey grid.

Data processing workflow and 3D inversion methodology

The basic processing of acquired time-domain measurements which results in frequency-domain data with noise estimates is described by Zach et al. (2008b). Consistent receiver timing is critical to obtain reliable phase information for azimuth data relative to inline data in the survey. The inline and

---

azimuth data recorded by a single receiver can then be collected and corresponding synthetic responses obtained in a single forward modelling in the reciprocal domain. The 3D inversion utilizes a fast finite-difference time-domain forward operator (Maaø, 2007), which provides synthetic fields and Green functions to be used by the gradient calculation and quasi-Newton optimization scheme described by Støren et al. (2008) and Zach et al. (2008a). The inversion software provides several regularization techniques, but to obtain the results shown here no regularizing terms were added to the data misfit functional.

Synthetic survey data

The synthetic survey data studied here were generated by forward modelling on an isotropic resistivity model having a sloping bathymetry from 1400 m to 2000 m, and containing three resistors. Figure 1 shows the resistor positions, and a contour plot of the seafloor. The naming convention A, B, and C is used to distinguish between the resistors. The resistors are homogeneous with resistivity 50 Ωm. The two larger resistors (B and C) are 50 m thick in the central parts and 25 m thick at the edges. They are buried at approximately 1300 m below the seabed. The smaller resistor (A) is 25 m thick and buried at about 850 m below seabed. Resistor A is very near resistor B, and delineation of these provides an additional challenge for the inversion. The seawater and background formation are homogeneous with resistivity 3.33 and 1 Ωm, respectively. We have generated various datasets representing typical survey layouts like 2D lines, coarse 3D scanning grids, and dense 3D grids. In the following, we will consider inversion results for some of these datasets.

Inversion of scanning dataset

A synthetic dataset with receiver and towline spacing of 4 km was input to the inversion, altogether 38 receivers and four towlines covering an area of 12x36 km^2. The survey layout with receiver positions and source towlines is indicated in Figure 1a. Note that none of the receiver positions and source towlines are located directly above the resistors. This complication makes inline-data only inversion unsuitable. Moreover, resistor C is completely outside of the receiver grid.

Inversion of the scanning grid dataset was carried out using the true background model as initial model. The input was inline and azimuth data at the frequency 0.25 Hz for both horizontal components of the electric field at offset ranges which would provide good signal-to-noise ratio in a real survey. Figure 2a and b show a vertical section and a depth slice of the resulting resistivity model. The lateral positions of the resistive regions reconstructed in the model agree with the positions of the true resistors. Resistors A and B are not completely delineated, but smear into a single high-resistive region. The resistor A reconstruction is deeper than the true model resistor. The lack of fine detail resolution in the reconstruction is due to the limited data coverage in the scanning dataset. As we will see later, the information contained in a denser 3D grid dataset is sufficient to give proper shape reconstruction and vertical delineation of resistors A and B. Note that resistor C is also partly reconstructed. Close to receiver positions, the edges of the resistor reconstructions display some jaggedness related to the lack of short offset data transverse to the source towlines. The reconstructed resistors are much thicker than the true resistors, but the resistivity-thickness product is comparable. The enlarged thickness effect could be compensated by regularization that provides forcing terms on the thickness of high-resistive volumes in the model.

In summary, the reconstruction using the scanning dataset lacks the fine details to properly determine vertical and lateral position of the resistors, but provides good anomalous resistivity detection and approximate locations. We emphasize that this is not the case for inversion using only the inline data, shown in Figure 2c). In this case the reconstruction of resistor B is split into two volumes following the towlines, and identification of the true resistor location between the lines is fortuitous. Moreover, there is no reconstruction of the smaller resistor A.
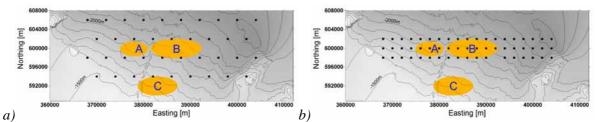
Figure 1 *True model resistors and bathymetry with receiver layout for a) scanning survey and b) denser 3D grid. Resistor depth below sea surface (approximate depth below seafloor): A 2500 m (850 m), B 3000 m (1300 m), C 2800 m (1300 m).*
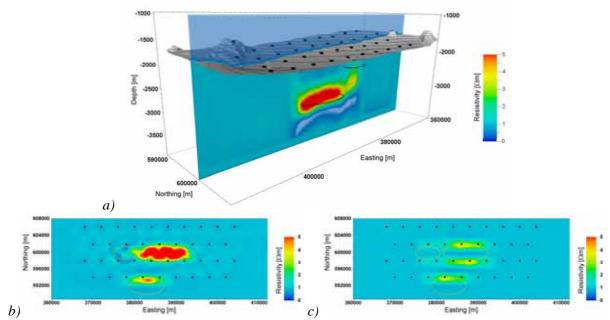

Figure 2 *Scanning dataset inversion including azimuth data in a) and b), and using inline data only in c). Fig. a) shows vertical section along resistors A and B with black polygons to outline the true model resistors, and b) shows a depth slice at 3000 m. c) Depth slice at 3200 m (strongest response).*
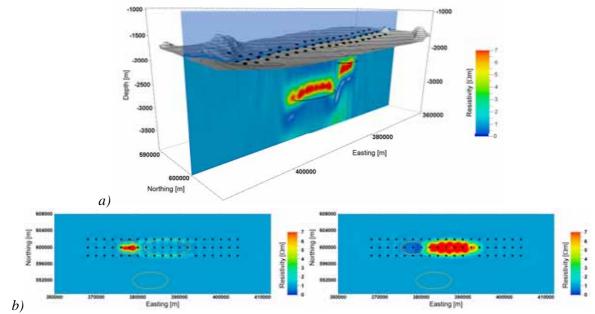

Figure 3 *Denser 3D grid dataset inversion result and receiver positions. a) Vertical section along resistors A and B with polygons that indicate outline of true model resistors. b) Depth slices at 2500 m and 2900 m.*

Denser 3D grid inversion

Based on the scanning data inversion, a natural extension of the survey to further determine the position of resistive volumes is the denser 3D grid outlined in Figure 1b. This survey layout consists of three survey lines with 2 km spacing both between towlines and between the receivers along the lines. In this survey, all three receiver lines record data for all source towlines. The resulting inversion resistivity model obtained from the same field and offset data input as in the scanning case is shown in Figure 3. In this case we used data at the frequencies 0.25 and 0.50 Hz. As we can see, resistors A and B are now delineated, and their position and thickness resolution have improved. The azimuth data have also in this case improved the result, as inversion of inline-data only (not shown) results in a less accurate horizontal and vertical positioning of the resistors.

Conclusions

We have shown 3D inversion results of synthetic CSEM data, and focus on the additional information provided by azimuth receiver measurements. When such data is included, inversion of coarse-grid scanning survey data is feasible, and provides detection of resistors between source towlines. The resulting resistivity models show the overall features of resistive bodies in the survey area. By developing a fast-track data processing workflow for real surveys, and running optimized inversion schemes that can give results within a few days, it could be possible to acquire a dense grid over identified interesting targets before the vessel has left the area. Such a dataset will in a subsequent inversion provide detailed information about resistor volume distributions, as demonstrated in the synthetic example shown here. An unconstrained inversion like this is typically the first step of an interpretation study integrating CSEM data with other information like seismic data.

References

Abubakar, A., Habashy, T.M., Druskin, V.L., Knizhnerman, L. and Alumbaugh, D. [2008] 2.5D forward and inverse modeling for interpreting low-frequency electromagnetic measurements. *Geophysics,* **73**, F165-F177.

Constable, S. and Srnka, L.J. [2007] An introduction to marine controlled-source electromagnetic methods for hydrocarbon exploration. *Geophysics,* **72**, WA3-WA12.

Jing, C., Green, K. and Willen, D. [2008] CSEM inversion: Impact of anisotropy, data coverage, and initial models. *SEG Expanded Abstracts* **27**, 604-608.

Maaø, F. A. [2007] Fast finite-difference time-domain modeling of marine-subsurface electromagnetic problems. *Geophysics*, **72**, A19–A23.

Mittet, R., Brauti, K., Maulana, H. and Wicklund, T.A. [2008] CMP inversion and post-inversion modelling for marine CSEM data. *First Break* **20**(8), 59-67.

Støren, T., Zach, J. J. and Maaø, F. [2008] Gradient calculations for 3D inversion of CSEM data using a fast finite-difference time-domain modelling code. *70th EAGE Conference & Exhibition,* Extended Abstracts, P194.

Suffert, J., Sangvai, P., Roth, F., Tyagi, A., and Bastia, R. [2008] Frontier exploration by electromagnetic scanning – A deep water example. *SEG Expanded Abstracts* **27**, 662-666.

Thrane, B.P., Meissner, E., Panzner, M. and Maaø, F.A. [2007] Effect of receiver density and azimuth data in grid modeling of seabed logging. *SEG Expanded Abstracts* **26**, 614-618.

Zach, J.J., Bjørke, A.K., Støren, T. and Maaø, F. [2008a] 3D inversion of marine CSEM data using a fast finite-difference time-domain forward code and approximate Hessian-based optimization. *SEG Expanded Abstracts* **27**, 614-618.

Zach, J. J., Roth, F. and Yuan, H. [2008b] Data preprocessing and starting model preparation for 3D inversion of marine CSEM surveys. *70th EAGE Conference & Exhibition,* Extended Abstracts, G003.